Science Advances
AAAS

Supplementary Materials for

The anti-fibrotic drug pirfenidone inhibits liver fibrosis by targeting the small oxidoreductase glutaredoxin-1

Yue Xi, Yanping Li, Pengfei Xu, Sihan Li, Zhengsheng Liu, Hung-chun Tung, Xinran Cai, Jingyuan Wang, Haozhe Huang, Menglin Wang, Meishu Xu, Songrong Ren, Song Li, Min Zhang, Yong J. Lee, Leaf Huang, Da Yang, Jinhan He*, Zhiying Huang*, Wen Xie*

*Corresponding author. Email: wex6@pitt.edu (W.X.); hzhiying@mail.sysu.edu.cn (Z.H.); jinhanhe@scu.edu.cn (J.H.)

Published 1 September 2021, *Sci. Adv.* **7**, eabg9241 (2021)
DOI: 10.1126/sciadv.abg9241

This PDF file includes:

Supplementary Materials:

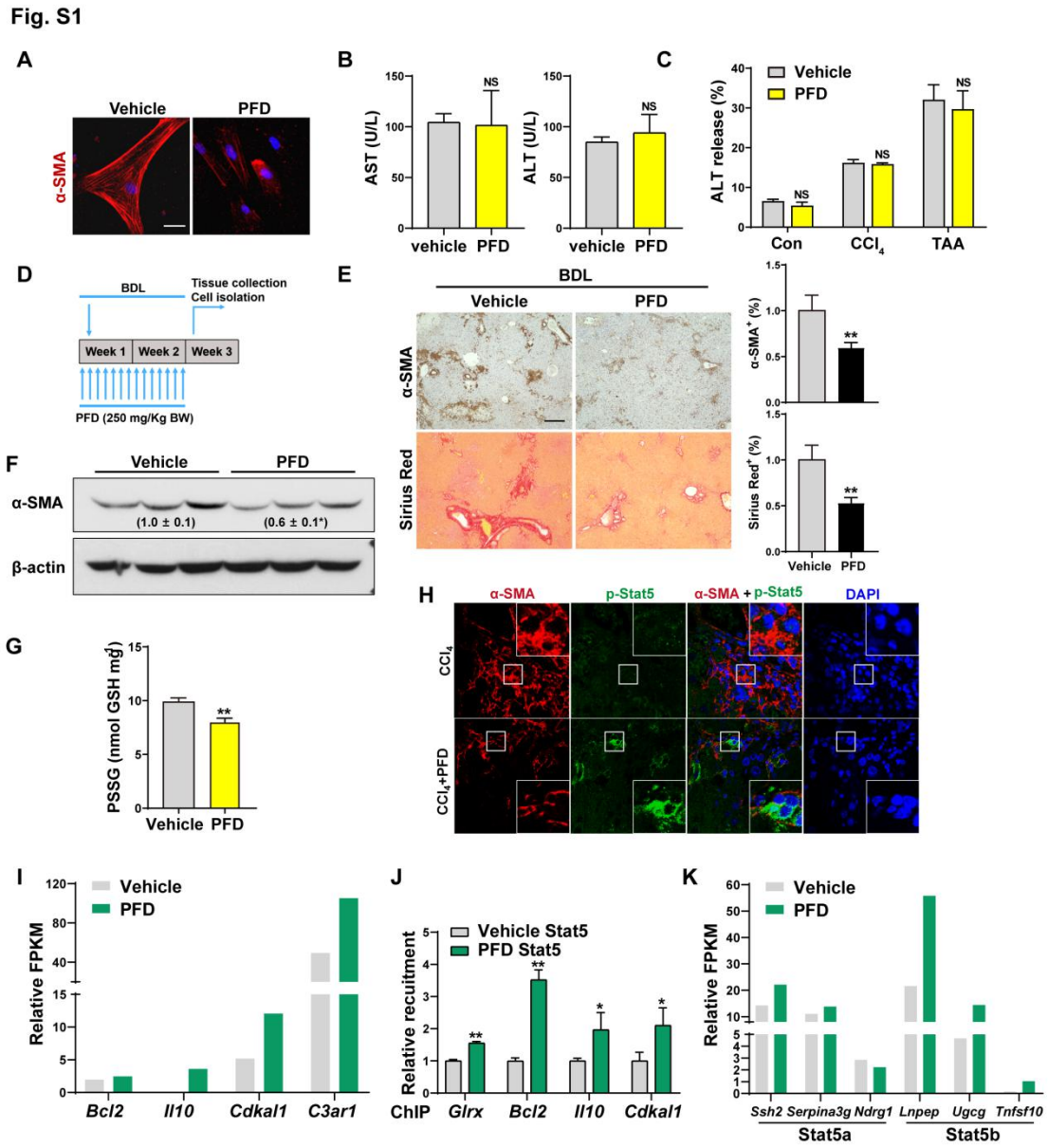

Fig. S1. PFD inhibits BDL-induced liver fibrosis and induces the expression of Glrx in a Stat5-dependent manner.

(**A**) Immunofluorescent staining of α-SMA (red) in primary human HSCs treated with vehicle or PFD (1 mM) for four days. Scale bar, 50 μm.

(**B**) The serum levels of AST and ALT in WT mice subjected to the CCl_4 model and treated with vehicle (n=4) or PFD (n=4).

(**C**) Primary hepatocytes isolated from WT mice treated with vehicle or PFD (1 mM) were treated with CCl_4 (800 uM) or TAA (100 mM) for 24h. The percentage of ALT release was measured (n=3).

(**D** to **F**) Eight weeks old male C57BL/6J mice subjected to BDL were treated with vehicle (n=4) or PFD (250 mg/kg body weight) (n=5) by gavage daily for two weeks as outlined in (**D**). Shown are immunostaining of α-SMA and Sirius Red staining with the quantifications shown on the right, scale bar, 200 μm (**E**), liver protein expression of α-SMA as measured by Western blotting with the relative quantification values labeled (**F**).

(**G**) Hepatic PSSG levels in WT mice subjected to the CCl_4 model and treated with vehicle (n=4) or PFD (n=4).

(**H**) Immunofluorescent staining of α-SMA and phosphorylated Stat5 in CCl_4-induced fibrotic livers. Shown in the larger boxes are magnified areas of corresponding smaller boxes.

(**I**) The expression of common Stat5 downstream genes by RNA-seq analysis of primary mouse HSCs treated with PFD (1 mM).

(**J**) ChIP assay to measure the recruitment of Stat5 onto the gene promoters of *Glrx* and Stat5 downstream genes in primary mouse HSCs (n=3).

(**K**) Stat5a- or Stat5b- dominating or specific downstream genes by RNA-seq analysis.

Data are shown as means ± S.D. *$p < 0.05$, **$p < 0.01$. Two-tailed Student's *t*-test.

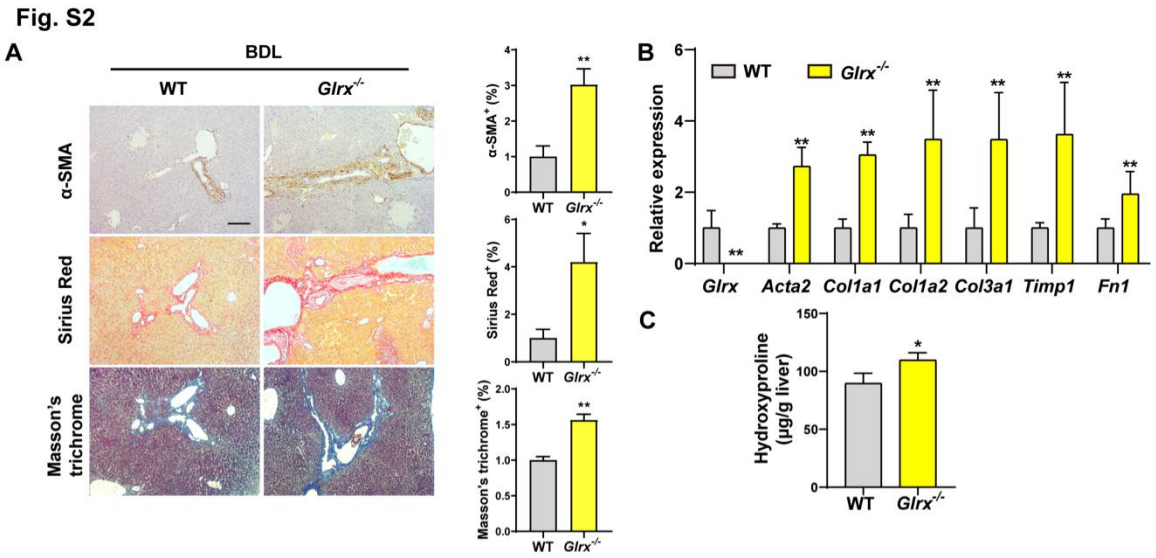

Fig. S2. *Glrx* ablation sensitizes mice to BDL-induced liver fibrosis.

(**A** to **C**) Eight weeks old male WT and *Glrx*$^{-/-}$ mice were subjected to BDL for two weeks (n=3 per group). Shown are α-SMA immunostaining, Sirius Red staining, and Masson's trichrome staining with the quantification shown on the right. Scale bar, 200 μm (**A**), the mRNA expression of *Glrx* and fibrogenic genes (**B**), and measurement of the liver content of hydroxyproline (**C**). Data are shown as means ± S.D. *p < 0.05, **p < 0.01. Two-tailed Student's *t*-test.

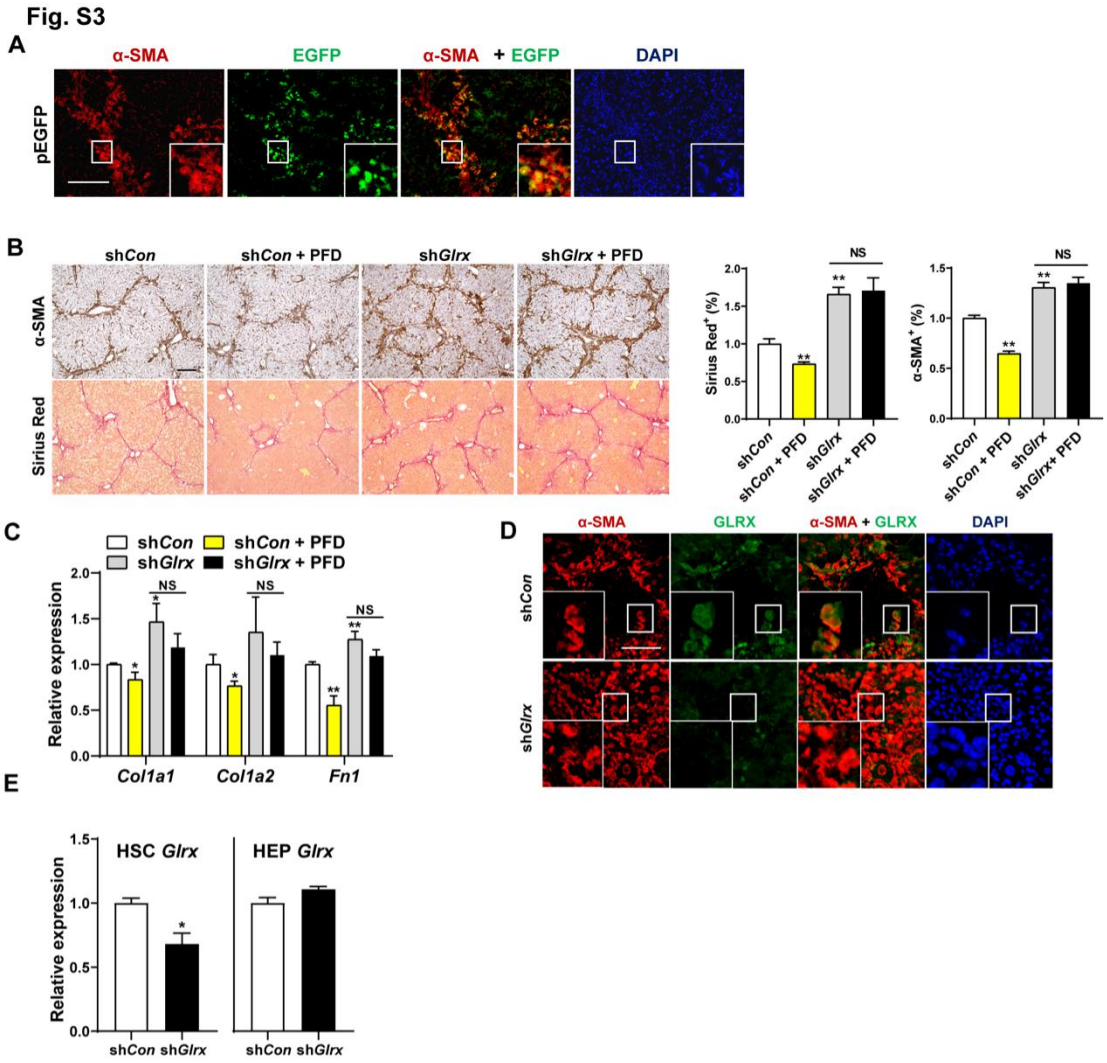

Fig. S3. Validation of the AEAA-conjugated nanoparticle delivery system by EGFP, and nanoparticle delivery of sh*Glrx* to HSCs sensitizes mice to liver fibrosis and abolishes the anti-fibrotic activity of PFD.

(**A**) Mice were subjected to a single injection of AEAA-conjugated nanoparticle loaded with EGFP expression plasmid after three weeks of CCl_4 treatment. Shown are EGFP expression and immunofluorescence staining of α-SMA (red) in fibrotic livers. Scale bar, 200 μm. Shown in the larger boxes are magnified areas of corresponding smaller boxes.

(**B** to **E**) Mice were subjected to the sh*Glrx* nanoparticle in the CCl_4 model. Shown are α-SMA immunostaining and Sirius Red staining with quantifications shown on the right (n=3), scale bar, 200 μm (**B**), hepatic mRNA expression of fibrogenic genes (n=3) (**C**), immunofluorescent staining of α-SMA and GLRX in fibrotic livers. Shown in the larger boxes are magnified areas of corresponding smaller boxes. Scale bar, 100 μm (**D**), and *GLRX* mRNA expression in primary HSCs and HEPs isolated from nanoparticle treated mice (n=3) (**E**).

Data are shown as means ± S.D. *$p < 0.05$, **$p < 0.01$. NS, statistically not significant. Data in **B** and **C** were analyzed by one-way analysis of variance with the Tukey's *post hoc* test. Data in **E** were analyzed by two-tailed Student's *t*-test.

Fig. S4

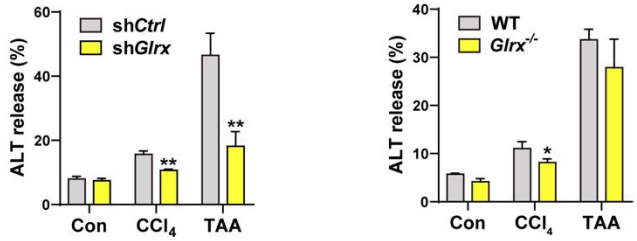

Fig. S4. GLRX depleted hepatocytes is less sensitive to CCl_4- or TAA-induced toxicity *in vitro*.

Primary hepatocytes isolated from WT mice infected with Ad-shCtrl or Ad-shGlrx (left), or primary hepatocytes isolated from WT or *Glrx*$^{-/-}$ mice (right) were treated with CCl_4 (800 uM) or TAA (100 mM) for 24h. The percentage of ALT release was measured (n=3).

Data are shown as means ± S.D. *$p < 0.05$, **$p < 0.01$. Two-tailed Student's *t*-test.

Fig. S5

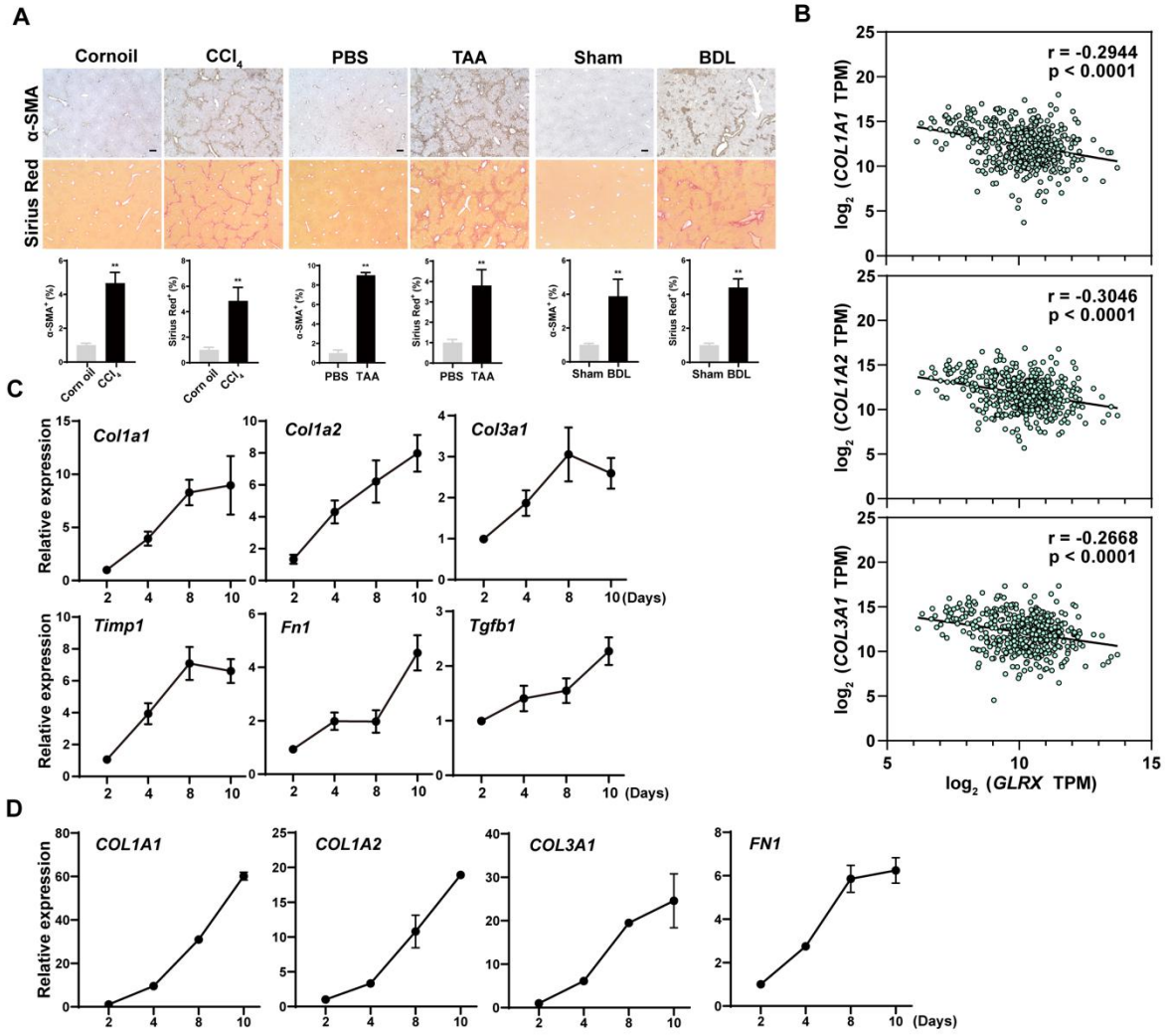

Fig. S5. The expression of *GLRX* inversely correlates with fibrogenic genes, and declines with the onset of activation in primary mouse and human HSCs.

(**A**) Immunostaining of α-SMA and Sirius Red staining in the CCl_4 model, TAA model , and the BDL model with the quantifications shown at the bottom (n=3 per group). Scale bar, 200 μm.

(**B**) Pearson correlation coefficient analysis of *GLRX* and *COL1A1*, *COL1A2*, or *COL3A1* expression in TCGA cohort of human livers (n=468).

(**C**) Gene expression in culture-activated primary mouse HSCs at indicated time points (n=3).

(**D**) Gene expression in culture-activated primary human HSCs at indicated time points (n=3).

Data are shown as means ± S.D. *p < 0.05, **p < 0.01. Two-tailed Student's *t*-test.

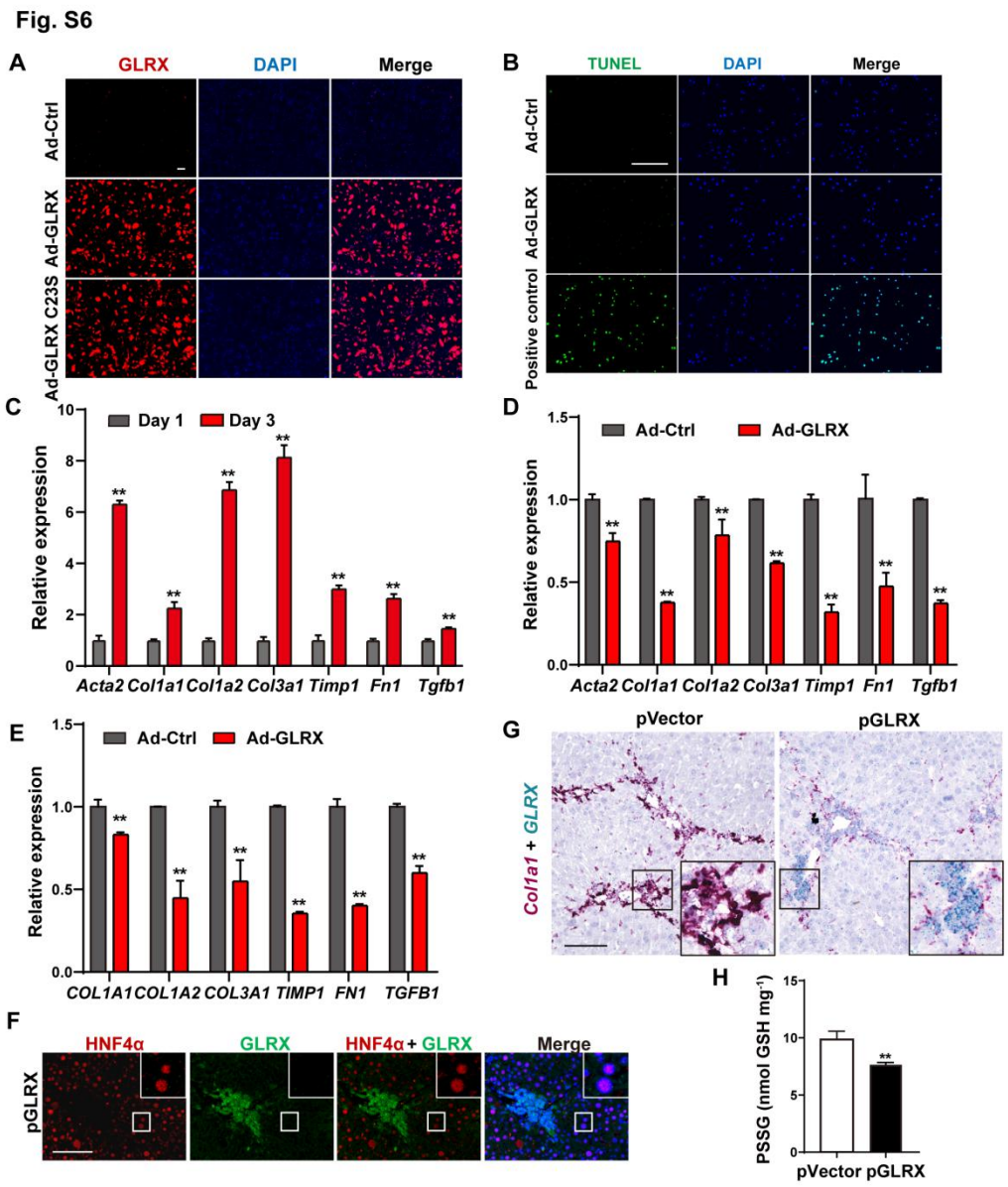

Fig. S6. Verification of GLRX and GLRX C23S expression, overexpression of GLRX reverses pre-existing HSC activation and liver fibrosis.

(**A** and **B**) Primary mouse HSCs were infected with Ad-GLRX or Ad-GLRX C23S one day after isolation and culture-activated for additional four days. Shown are immunofluorescent staining of GLRX (red), scale bar, 200 μm (**A**), and TUNEL staining, scale bar, 200 μm (**B**). HSCs treated with recombinant DNase I were used as the positive control.

(**C**) Fibrogenic gene expression in primary mouse HSCs culture-activated for three days (n=3).

(**D**) Culture-activated HSCs in **c** were then infected with Ad-Ctrl or Ad-GLRX and cultured for three additional days before gene expression analysis (n=3).

(**E**) Gene expression was measured in Ad-Ctrl or Ad-GLRX infected pre-activated passage 5 human HSCs (n=3).

(**F**) Immunofluorescence staining of GLRX (green) and hepatocyte marker HNF4α (red) in fibrotic livers. Scale bar, 200 μm. Shown in the larger boxes are magnified areas of corresponding smaller boxes.

(**G**) RNA in situ hybridization (ISH) of *Col1a1* and *GLRX* in fibrotic livers. Scale bar, 200 μm. Shown in the larger boxes are magnified areas of corresponding smaller boxes.

(**H**) PSSG levels in livers of mice subjected to the GLRX nanoparticle regimen (n=4).

Data are shown as means ± S.D. *$p < 0.05$, **$p < 0.01$. Two-tailed Student's *t*-test.

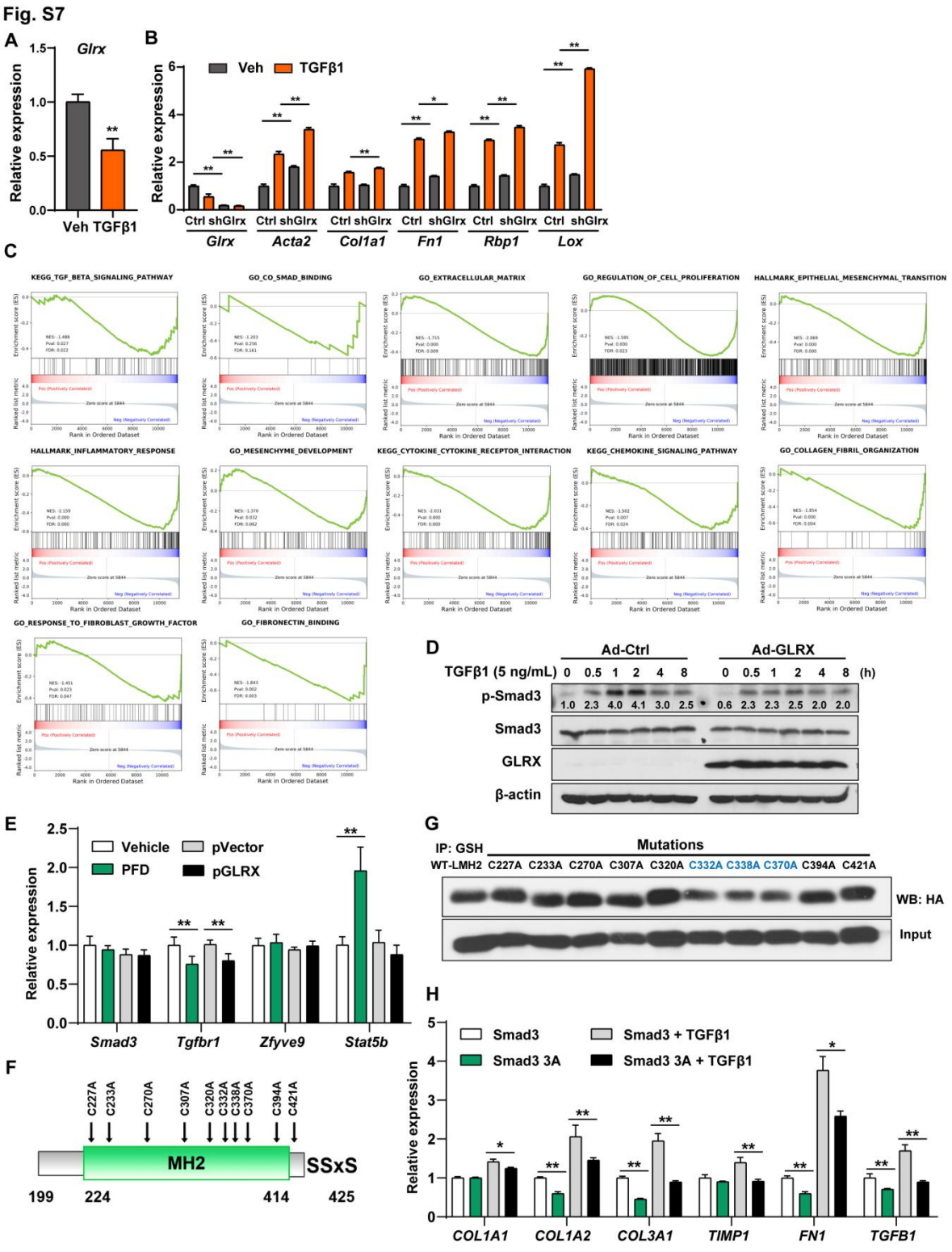

Fig. S7. GLRX Knockdown exacerbates TGFβ-stimulated HSC activation, and Smad3 is a novel GLRX substrate.

(**A**) *Glrx* expression in primary mouse HSCs treated with TGFβ1 (4 ng/mL).

(**B**) Primary mouse HSCs infected with Ad-shCtrl or Ad-shGlrx were treated with TGFβ1 (4 ng/mL) before gene expression analysis (n=3).

(**C**) RNA-seq analysis on primary mouse HSCs infected with Ad-GLRX or Ad-Ctrl. Shown is GSEA of gene related clusters of TGFβ Signaling Pathway, Co-Smad Binding, Extracellular Matrix, Cell Proliferation, Epithelial Mesenchymal Transition, Inflammatory Response, Mesenchyme Development, Cytokine and Cytokine Receptor Interaction, Chemokine Signaling Pathway, Collagen and Fibril Organization, Response to Fibroblast Growth Factor, and Fibronectin Binding.

(**D**) The phosphorylation of Smad3 in LX2 cells infected with Ad-GLRX was assessed by Western blotting with the relative p-Smad3 values labeled.

(**E**) Gene mRNA expression in HSCs isolated from CCl_4-treated mice subjected to PFD treatment or GLRX nanoparticle regimen (n=3).

(**F**) Schematic illustration of the 10 cysteines in the L-MH2 domain.

(**G**) LX2 cells were transfected with WT HA-L-MH2 or mutant HA-L-MH2 with the 10 cysteines mutated to alanines individually. PSSG of L-MH2 was determined by IP with an anti-GSH antibody followed by Western blotting.

(**H**) LX2 cells transfected with Smad3 or Smad3 3A expression plasmid were stimulated by TGFβ1 (5 ng/mL) for 24 h before assessing fibrogenic gene expression.

Data are shown as means ± S.D. *$p < 0.05$, **$p < 0.01$. Data in **A** were analyzed by two-tailed Student's *t*-test. Data in **B, E,** and **H** were analyzed by one-way analysis of variance with the Tukey's *post hoc* test.

Table S1. Real-time PCR Primer Sequences

Gene names	Forward sequences (5'-3')	Reverse sequences (5'-3')
Glrx	AACAACACCAGTGCGATTCA	ATCTGCTTCAGCCGAGTCAT
Acta2	TGAAGATCCTGACTGAGCGT	TGATGTCACGGACAATCTCA
Col1a1	ACTGCAACATGGAGACAGGTCAGA	ATCGGTCATGCTCTCTCCAAACCA
Col1a2	GAGGACTTGTTGGTGAGCCT	CTCACCCTTGTTACCGGATT
Col3a1	CTGTAACATGGAAACTGGGGAA	CCATAGCTGAACTGAAAACCACC
Timp1	GGTGTGCACAGTGTTTCCCTGTT T	TCCGTCCACAAACAGTGAGTGTCA
Fn1	GATGTCCGAACAGCTATTTACCA	CCTTGCGACTTCAGCCACT
Tgfb1	CTGAACCAAGGAGACGGAAT	TTGCTGTCACAAGAGCAGTG
Tgfbr1	TGATCCATCGGTTGAAGAAA	TGGCATACCAGCATTCTCTC
Rbp1	TGTGGACTTCAACGGGTACTGG	TTGTCTGGCTTCAGCAAGTTGG
Lox	CACAGAGGAGAGTGGCTGAA	AATCCCTGTGTGTGTGCAGT
Pparg	GGAATCAGCTCTGTGGACCT	GTGGAGCAGAAATGCTGGAG
Grap	GTACTCGGGCAGGATCTCTC	TCACAGAGACGGAGAACTCG
Lrat	TCACCTAGACGGGACTCTCA	CGCAGTTGTTCCACAGTAGG
Cyclophilin	GGAGATGGCACAGGAGGAA	GCCCGTAGTGCTTCAGCTT
β-actin	CGGTTCCGATGCCCTGAGGCTCTT	CGTCACACTTCATGATGGAATTGA
GLRX	GCCCAAGAGATCCTCAGTCA	CCCGTGAGCTGTTGCAAATA
ACTA2	AAGAGGAATCCTGACCCTGAA	TGGTGATGATGCCATGTTCT
COL1A1	CGGTGTGACTCGTGCAGC	ACAGCCGCTTCACCTACAGC
COL1A2	TCAAACTGGCTGCCAGCAT	CAAGAAACACGTCTGGCTAGG

COL3A1	CCCAGGGAAAGATGGCCCAA	CTCACCAGGGCTACCACGAG
TIMP1	TCTGCAATTCCGACCTCGTCATCA	AAGGTGGTCTGGTTGACTTCTGGT
FN1	GCACCTGATGGTGAAGAAGA	GGAATAGCTGTGGACTGGGT
TGFB1	CGCTAAGGCGAAAGCCCTCAATTT	ACAATTCCTGGCGATACCTCAGCA
CYCLOPHILIN	CCTAAAGCATACGGGTCCTGGCA	CACATGCTTGCCATCCAACCACT
β-ACTIN	AGGCACCAGGGCGTGAT	GCCCACATAGGAATCCTTCTGAC